Environmental Science & Technology Letters

pubs.acs.org/journal/estlcu

Letter

Open Access

This article is licensed under CC-BY 4.0

Effect of AC Field Frequency on Membrane Colloidal Deposition and Detachment

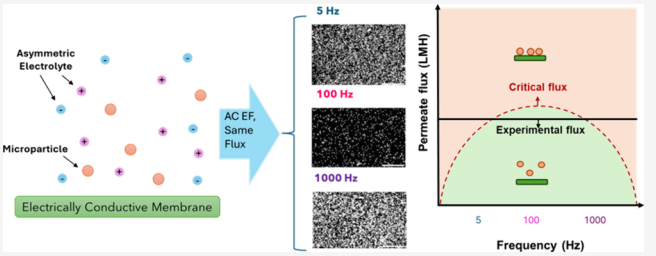
Elina Yachnin, Fan Yang, David Jassby, Eric M. V. Hoek, Tamar Segal-Peretz, and Guy Z. Ramon*

Cite This: https://doi.org/10.1021/acs.estlett.5c00623

Read Online

ACCESS | Metrics & More | Article Recommendations | Supporting Information

ABSTRACT: Colloidal fouling remains an operational challenge for numerous membrane filtration processes. While various approaches exist for fouling mitigation, the use of time-periodic electric fields represents a particularly interesting, relatively unexplored one. Here, we report experimental results of colloidal deposition onto an electrically conductive membrane in the presence of AC electric fields of varying frequency. We show that fouling mitigation can be achieved in the presence of an AC electric field at a relatively low applied potential amplitude of 1 V. Moreover, an extremum in the frequency response is observed in the medium frequency range (represented by 100 Hz), where deposition is greatly reduced with slow kinetics and remains reversible, all while maintaining constant permeate flux. Our results serve as an initial, experimental proof of concept, demonstrating the potential of tuning AC fields for fouling control.



KEYWORDS: *ultrafiltration, microfiltration, colloidal fouling, electrically conducting membrane, AC electric field*

Downloaded via 185.104.138.116 on July 27, 2025 at 14:16:15 (UTC).
See https://pubs.acs.org/sharingguidelines for options on how to legitimately share published articles.

INTRODUCTION

Ultrafiltration (UF) and microfiltration (MF) membranes are used for a range of separation processes, from water and wastewater treatment to biotech, pharmaceuticals, food, automotive, and high tech.[1−3] However, membrane fouling remains a significant challenge, hindering efficient operation.[4−6] Foulants, such as inorganic colloidals, macromolecules, or biomass, accumulate on the membrane surface, increasing hydraulic resistance and, therefore, operational costs due to the higher energy input and frequent maintenance, which can also reduce the membrane lifespan.[4,7] Current strategies to decrease the rate and extent of membrane fouling include feed pretreatment, operational optimization backwashing, and surface modifications.[4,6,8,9] However, since the fouling process is a complex combination of physical and chemical interactions between the membrane material and various foulants, fouling remains a persistent issue and effective solutions are still needed.

Use of electric fields has been demonstrated as a means to control fouling via various mechanisms, such as electrophoresis, dielectrophoresis, and electroosmosis.[10−12] To date, these have primarily focused on direct current (DC), applied to a variety of membrane−foulant systems, presenting successful fouling mitigation through mechanisms of increased electrostatic repulsion[13−16] and the promotion of detachment via electrochemical reactions.[17−21]

The use of alternating current (AC) offers potential benefits over DC in addressing some of its key limitations, namely, reducing Joule heating and minimizing electrochemical reactions that lead to membrane deterioration and the release of chemical species into the treated water. Thus, AC application may provide a more energy-efficient and practical approach to fouling control.[21−23] However, far less has been reported on AC application, warranting further research into the mechanisms at play and their potential for fouling mitigation. When an AC field is applied, frequency dependence adds an inherent layer of complexity. Previous studies have offered some insights to the effect of the AC field on microparticles near a rigid metal electrode.[24−26] In an asymmetric electrolyte with different ion diffusivities-arising from differences in ion charge or mobility, the diffusivity mismatch is defined as $\delta = \frac{D_-}{D_+} \neq 1$, where D_- and D_+ are the diffusivities of the anion and cation, respectively. It was shown that, in the presence of an oscillating electric field, this diffusivity mismatch leads to the formation of a long-range electric field that can counteract gravity, resulting in the levitation of microparticles up to several micrometers above the electrode surface.[24]

In the context of membrane fouling, the effect of low-frequency AC fields on the fouling of commercial (non-

Received: June 24, 2025
Revised: July 15, 2025
Accepted: July 16, 2025

© XXXX The Authors. Published by American Chemical Society

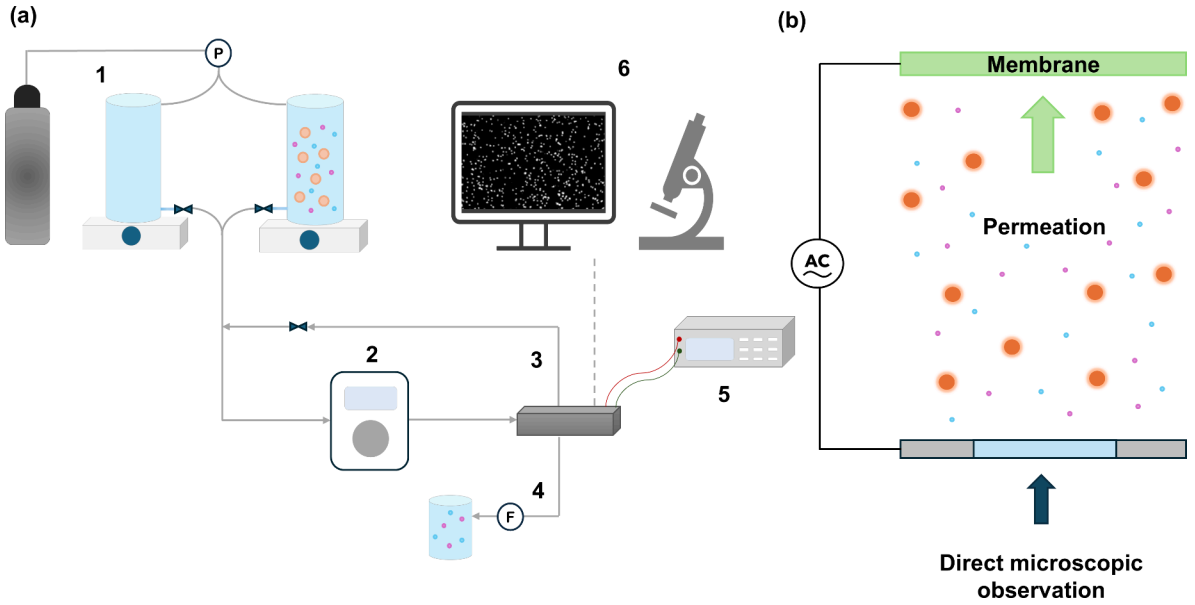


Figure 1. (a) Schematic illustration of the experimental system: (1) Fouling and cleaning solutions are pressurized with N_2 to a pressure according to the desired permeate flux through the membrane, using a pressure controller. Fouling solution consists of the model foulant microparticles (orange) and the model electrolyte (blue and purple), (2) pump, (3) flow cell, (4) flow meter for the permeate, (5) signal generator, and (6) confocal microscope. (b) Schematic side view inside the flow cell, where the direct microscopic observation is performed using an inverted microscope and the membrane is located at the upper part of the flow cell and acts as an electrode.

electrically conductive) ultrafiltration membranes by bovine serum albumin was studied,[27] concluding that low frequency and high field strength are optimal for reducing membrane fouling. To further understand the mechanism of fouling mitigation using AC fields, a recent study by Bhattacharjee et al.[23] numerically calculated the time-averaged electric field near the surface of an electrically conducting membrane, demonstrating that the critical flux is maximized for a specific resonant frequency. Above the critical flux, the propensity for fouling dramatically increases, primarily due to the increase in the permeate drag force.[28−30]

Herein, we experimentally show that the critical flux near an electrically conductive UF membrane can be controlled through the application of a finely tuned AC field. Specifically, a minimum initial deposition rate and maximum release of a model foulant (polystyrene microparticles) are achieved at ∼100 Hz, consistent with the existence of a resonant frequency within this range. The fouling solution contained an asymmetric model electrolyte (sodium hydroxide, $\delta = 4$), chosen to increase the repulsive electric forces between the negatively charged particles and the electric field. As $\delta \neq 1$, a non-zero time-average electric field is formed when AC is applied, with negative peaks forming over the range of several micrometers.[23−25,31] Thus, the interplay between the formed electrodynamic, frequency-dependent force and the permeate drag leads to an increased critical flux, resulting in a wider range of operating fluxes with lower fouling propensity.

MATERIALS AND METHODS

Electrically Conductive Membranes. Ultrafiltration electrically conductive membranes were fabricated based on a previously published method by Dudchenko et al.[16] In short, the CNT−COOH suspension was pressure-deposited onto a PS-35 membrane support and cross-linked in a heated, acidic environment. The average membrane water permeability of the coupons (38 × 8 mm^2) was ∼40 LMH/bar. The measured electric potential difference between the membrane and the counter electrode was 0.95 V (see Figure S1 of the Supporting Information).

Feed Solution. The feed consisted of a background asymmetric electrolyte (1 mM NaOH, Sigma-Aldrich) and a model colloid (carboxylated polystyrene particles, 1 μm diameter, 10^6 particles/mL, excitation/emission at 540/560 nm, respectively, Thermo Fisher). It should be noted that the type of electrolyte in the feed stream substantially affects the developed electric field. NaOH was chosen as it amplifies the AC field frequency effect due to its high diffusivity asymmetry ($\delta \sim 4$) and enhances the observation and analysis of the underlying mechanism. This effect is reduced when an electrolyte with a lower δ is present in the solution, such as NaCl ($\delta \sim 1.33$), which is a common constituent of natural waters. Nevertheless, the effect persists and may still be substantial, as discussed in detail by Bhattacharjee et al.[23] and Hashemi et al.[23,24,31]

Experimental Setup. The feed solution was pressurized with N_2 and circulated with a gear pump (Cole-Parmer) through a custom-made flow cell (sized 38 × 8 × 0.6 mm) that enabled *in situ* visualization of the membrane surface during the filtration process under an applied electric field. A sinusoidal electric signal with an amplitude of 1 V (∼16 V/cm) was applied at varying frequencies by using a signal generator (Rigol) and monitored by using a multimeter. The flux during fouling experiments was maintained using a flow sensor connected to a pressure regulator (Fluigent). Double distilled water (DDW) were circulated from an additional vessel during the cleaning procedure. Images of the membrane surface were taken with a confocal microscope (TCS-SP8, Leica Microsystems), as described in previous studies.[32−34] A schematic diagram of the system and an internal view of the flow cell are presented in Figure 1.

Fouling and Cleaning Procedures. The experiments were conducted under a constant flux of 47 LMH in dead-end

https://doi.org/10.1021/acs.estlett.5c00623
Environ. Sci. Technol. Lett. XXXX, XXX, XXX−XXX

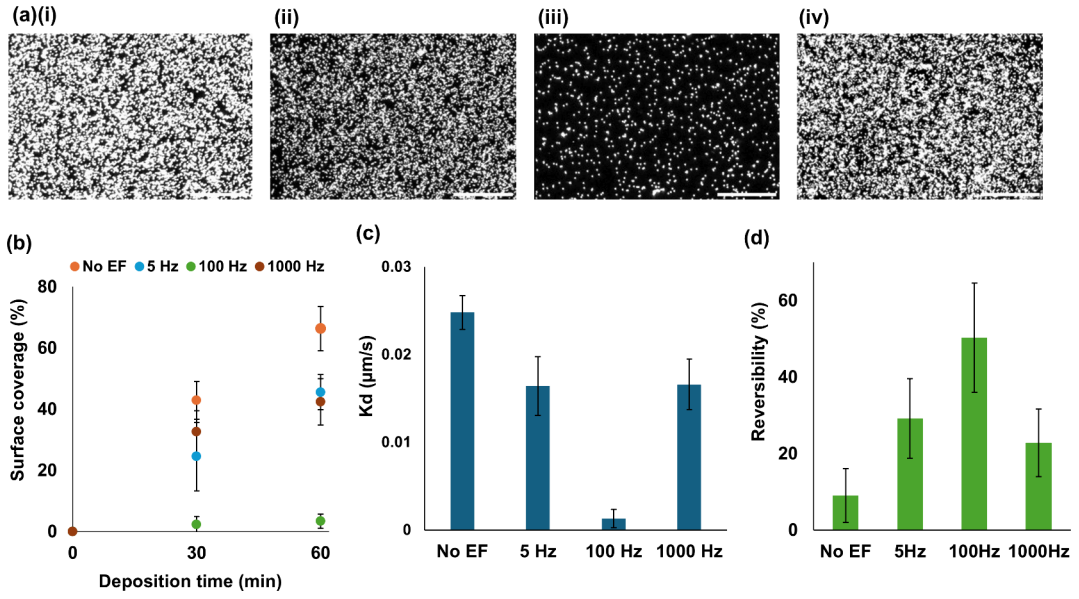


Figure 2. (a) (i–iv) Confocal images of the microparticulate deposition on the electrically conductive membrane, where (i) no AC field was applied versus an amplitude of 1 V was applied at frequencies of 5, 100, and 1000 Hz (ii, iii, and iv, respectively). Image scale bars are 50 μm. (b) Colloidal deposition after 30 and 60 min. (c) Respective deposition rate coefficients for deposition after 60 min. (d) Deposition reversibility at frequencies of 5, 100, and 1000 Hz and without an AC field. Standard deviations were calculated based on the average of three repetitions at three different locations.

mode (to generate severe deposition) in three steps: (1) permeability test with DDW, (2) fouling experiment with pressurized feed solution with or without an applied electric field, and (3) cleaning procedure with DDW, without an applied pressure and electric field. Images of the membrane surface ($140 \times 200\ \mu m^2$) were taken at three separate locations at t = 0.30 and 60 min as well as following the cleaning cycle, conducted by a simple physical rinse with DDW under a crossflow rate of 15 mL/min (0.05 m/s) for 5 min.

In the images, the membrane is the black background, while the deposited particles are white. Surface coverage (as % of the total) was calculated using ImageJ. Each experiment was repeated 3 times to ensure reproducibility. Mean surface coverage (%) and the standard deviation, for each condition, were calculated based on 9 measurements. The degree of reversibility for the observed deposition was determined as

$$r = 1 - \frac{A_{wash}}{A_{dep}} \quad (1)$$

where A_{wash} and A_{dep} are the surface coverage after the cleaning procedure and at the end of the deposition experiment (after 60 min), respectively.

RESULTS AND DISCUSSION

We examined colloidal deposition of the model solution with and without the presence of an AC field [frequencies of 5 Hz (low), 100 Hz (intermediate), and 1000 Hz (high)], in order to explore the frequency response and prove that it has a "maximum", for which deposition is minimal, and the detachment is highest. This would imply that the system is within proximity to the resonant frequency that was theoretically predicted in previous studies.[23] First, we investigated the effect of the AC field on deposition kinetics. Representative confocal images of deposited particles on the membrane surface after 60 min are presented in Figure 2a (i–iv). Corresponding particulate surface coverage after 30 and 60 min of deposition is presented in Figure 2b. In the experiments, the highest deposition was observed when no AC was applied (~45% after 30 min and ~65% after 1 h). While all three applied AC frequencies resulted in reduced surface coverge after both time points, a significant trend was observed, with a clear minimum at 100 Hz. The application of AC at the intermediate frequency (100 Hz) resulted in a very low colloidal deposition observed (~3.5% after 30 min and ~5% after 1 h). At low and high frequencies (5 and 1000 Hz), conversely, the surface coverage was reduced by only ~21 and ~24%, respectively. We note that the standard deviation can largely be attributed to the inhomogeneities of the membrane coupons, resulting in potentially large, localized permeation rates. Nevertheless, the observed trends of surface coverage remain consistent with the AC frequency.

To further understand the fouling behavior under the applied AC field, the deposition rate coefficient, k_d, is calculated as[17,35,36]

$$k_d = \frac{\theta(t)}{\Delta t \cdot N_0 \cdot A_p} = \frac{\theta(t)^*}{\Delta t} \quad (2)$$

where $\theta(t)/\Delta t$ is the surface coverage percentage of particles attached to the membrane per time, A_p is the surface area of a single particle (μm^2), and N_0 is the number of microparticles in the bulk (number/μm^3). For derivation, see eqs S1 and S2 in the Supporting Information. k_d is calculated from the slope of the normalized surface coverage percentage $\theta(t)^*$ plotted with time (see Figure S2 of the Supporting Information). According to Figure 2c, k_d follows the same trend: it is highest when no electric field was applied and lowest at 100 Hz. This shows a maximum in the frequency response, implying proximity to the resonance frequency, affecting the kinetics of the deposition process.

We hypothesized that the AC-induced repulsive force affects not only the deposition of the microparticles but also their ability to detach from the surface when the permeate flux and

https://doi.org/10.1021/acs.estlett.5c00623
Environ. Sci. Technol. Lett. XXXX, XXX, XXX−XXX

the electric field are turned off. To study the reversibility, we analyzed the surface coverage after a washing procedure at the end of each fouling experiment. Image analysis of the surface coverage in Figure 2d shows that, without AC field application, the average deposition reversibility was 9%. However, application of the AC field with a frequency of 100 Hz resulted in a 50% increase of the uncovered surface. The proposed explanation for this observation is that application of the AC field leads to the development of a long-range (on the scale of micrometers or more), time-averaged electrodynamic force, arising from the response of the asymmetric electrolyte to the AC field. This force, when applied at the appropriate frequency, can overcome the permeate drag force, hence effectively increasing the critical flux and the reversibility of particle deposition. The relation between the critical flux and deposition reversibility was established in previous studies:[30,36−39] irreversible deposition occurs when operating above the critical flux, where the drag force exceeds the repulsive electrostatic or acid−base interactions (XDLVO theory). In a similar fashion, the repulsive time-averaged electrodynamic force is added to the force balance and reduces the propensity for deposition and adhesion of the particles to the membrane, effectively bringing the system to below the critical flux, though the operating flux remains constant.

To further explain the results, we present a schematic illustration of equilibrium positions versus permeate flux and frequency (see Figure 3a). Here, we distinguish between stable

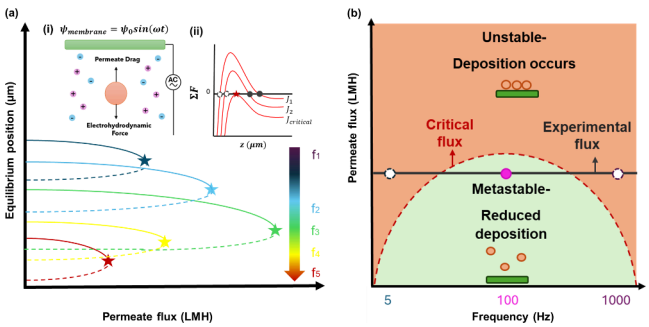


Figure 3. Schematic illustrations: (a) Equilibrium positions at various distances from the membrane vs permeate flux and frequencies ($f_1 < f_2 < f_3 < f_4 < f_5$).[23] (Star) Critical permeate flux. Inset: (i) Force balance on a microparticle and (ii) total force vs distance from the membrane for various permeate fluxes J ($J_1 < J_2 < J_{critical}$) at a constant frequency, with stable (●) and unstable (○) equilibrium positions shown, at $\sum F = 0$. (b) Proposed phase diagram for colloidal fouling in the presence of an AC field: permeate flux vs frequency. The dotted line is the critical flux, above which the drag force is increased and deposition occurs. Below the critical flux, there is a metastable equilibrium. The applied frequency dictates whether the experimental flux is above or below the critical flux.

and unstable equilibrium positions (for which $\sum F = 0$), where two equilibrium positions are obtained for each permeate flux at values below the critical flux. Each line in Figure 3a represents the equilibrium positions at a given frequency and permeate flux, with stable equilibrium positions represented with solid lines and unstable ones represented with dotted lines. The intersection of these lines is the critical flux. At the critical flux and beyond, no equilibrium position exists [Figure 3a (ii)], as the drag force dominates and deposition occurs.[23,28−30] The critical flux possesses a maximum for a resonant frequency.[23] This can be translated into a phase diagram, presented in Figure 3b, that describes the critical flux dependence on the frequency and consists of two regions with respect to particle deposition: unstable and metastable. The unstable region is located above the critical flux, where the electrodynamic force is insufficient to resist the permeate drag, leading to an increased and irreversible particulate deposition on the membrane. The metastable region is below the critical flux, where the electrodynamic force is equal or exceeds the permeate drag, enabling the particles to levitate further from the membrane and mitigate the colloidal deposition. The transition between these regions can be achieved through frequency tuning, which affects the movement of the electrolyte as a response to the AC field. At high frequencies, the electrolyte cannot effectively follow the oscillating electric field, resulting in minimal translational displacement and consequently a reduced long-range electric field. At sufficiently low frequencies, the slow oscillations allow the electrolyte to reorganize in response to the local charge near each electrode. This reduces the AC effect of the long-range electric field as the system approaches quasi-DC behavior. In both high- and low-frequency regimes, the dominant forces acting on the colloids are the hydrodynamic drag, van der Waals attraction, and electric double-layer repulsion. It is only within the intermediate frequency range that field oscillations are fast enough to prevent full ionic rearrangement but slow enough to sustain a time-averaged long-range electric field. Under these conditions, this field acts as an effective repulsive force, increasing the critical flux and mitigating colloidal deposition on the membrane surface.

Our results suggest that for a range of resonant frequencies the working flux in the filtration process is below the critical flux and the probability for colloidal deposition is decreased. Frequencies outside this range will not mitigate deposition as effectively as the working flux will be above the critical flux. Variation of the AC field frequency enables the crossing between both regions, so that deposition will be reduced while maintaining a constant permeate flux during the filtration process.

To conclude, this work experimentally demonstrated how applying an AC field with a frequency within the range of the resonant frequency can significantly reduce the initial colloidal deposition on electrically conductive membranes. The electrolyte was chosen according to its diffusivity mismatch value δ and the foulant charge: for a negatively charged foulant, electrolyte with $\delta > 1$ was used to develop a negatively charged, repulsive AC field that leads to decreased deposition kinetics and reversible deposition processes. The frequency of the AC field plays an important role in mitigating colloidal deposition, as an extremum in the frequency response was experimentally identified at which colloidal deposition is minimized while the permeate flux remains constant. This approach can enable the treatment of a wide range of foulants by adjusting the properties of the asymmetric electrolyte. The results provide experimental proof of concept of the impact AC fields on fouling mitigation and, importantly, demonstrate their tunability. These findings lay the groundwork for further studies under more realistic operational conditions.

■ ASSOCIATED CONTENT

Supporting Information

The Supporting Information is available free of charge at https://pubs.acs.org/doi/10.1021/acs.estlett.5c00623.

https://doi.org/10.1021/acs.estlett.5c00623
Environ. Sci. Technol. Lett. XXXX, XXX, XXX−XXX

Measurment of frequencies and amplitudes (Figure S1), colloidal deposition rate calculation (Figure S2), and derivation of eq 2 (PDF)

AUTHOR INFORMATION

Corresponding Author

Guy Z. Ramon − *Department of Civil and Environmental Engineering, Technion—Israel Institute of Technology, Haifa 3200003, Israel; Department of Chemical Engineering, Technion—Israel Institute of Technology, Haifa 3200003, Israel;* orcid.org/0000-0002-0711-0654; Email: ramong@technion.ac.il

Authors

Elina Yachnin − *Department of Civil and Environmental Engineering, Technion—Israel Institute of Technology, Haifa 3200003, Israel*

Fan Yang − *Department of Civil and Environmental Engineering, University of California, Los Angeles, Los Angeles, California 90095-1593, United States;* orcid.org/0000-0001-6319-6053

David Jassby − *Department of Civil and Environmental Engineering, University of California, Los Angeles, Los Angeles, California 90095-1593, United States;* orcid.org/0000-0002-2133-2536

Eric M. V. Hoek − *Department of Civil and Environmental Engineering, University of California, Los Angeles, Los Angeles, California 90095-1593, United States; Energy Storage & Distributed Resources Division, Lawrence Berkeley National Laboratory, Berkeley, California 94720, United States;* orcid.org/0000-0002-5748-6481

Tamar Segal-Peretz − *Department of Chemical Engineering, Technion—Israel Institute of Technology, Haifa 3200003, Israel;* orcid.org/0000-0003-3222-6429

Complete contact information is available at: https://pubs.acs.org/10.1021/acs.estlett.5c00623

Notes

The authors declare no competing financial interest.

ACKNOWLEDGMENTS

This research was supported by the U.S.−Israel Binational Science Foundation (BSF, Grant 2019603) and the Israel Science Foundation (ISF, Grant 3041/21).

REFERENCES

(1) Lee, S.; Ihara, M.; Yamashita, N.; Tanaka, H. Improvement of virus removal by pilot-scale coagulation-ultrafiltration process for wastewater reclamation: Effect of optimization of pH in secondary effluent. *Water Res.* **2017**, *114*, 23−30.

(2) Mohammad, A. W.; Ng, C. Y.; Lim, Y. P.; Ng, G. H. Ultrafiltration in Food Processing Industry: Review on Application, Membrane Fouling, and Fouling Control. *Food Bioprocess Technol.* **2012**, *5*, 1143−1156.

(3) Al Aani, S.; Mustafa, T. N.; Hilal, N. Ultrafiltration membranes for wastewater and water process engineering: A comprehensive statistical review over the past decade. *J. Water Process. Eng.* **2020**, *35*, 101241.

(4) Gao, W.; et al. Membrane fouling control in ultrafiltration technology for drinking water production: A review. *Desalination* **2011**, *272*, 1−8.

(5) She, Q.; Wang, R.; Fane, A. G.; Tang, C. Y. Membrane fouling in osmotically driven membrane processes: A review. *J. Membr. Sci.* **2016**, *499*, 201−233.

(6) Guo, W.; Ngo, H. H.; Li, J. A mini-review on membrane fouling. *Bioresour. Technol.* **2012**, *122*, 27−34.

(7) Nthunya, L. N.; et al. Fouling, performance and cost analysis of membrane-based water desalination technologies: A critical review. *J. Environ. Manage.* **2022**, *301*, 113922.

(8) Shi, X.; Tal, G.; Hankins, N. P.; Gitis, V. Fouling and cleaning of ultrafiltration membranes: A review. *J. Water Process. Eng.* **2014**, *1*, 121−138.

(9) Hilal, N.; Ogunbiyi, O. O.; Miles, N. J.; Nigmatullin, R. Methods employed for control of fouling in MF and UF membranes: A comprehensive review. *Sep. Sci. Technol.* **2005**, *40*, 1957−2005.

(10) Shen, Y.; Badireddy, A. R. A Critical Review on Electric Field-Assisted Membrane Processes: Implications for Fouling Control, Water Recovery, and Future Prospects. *Membranes* **2021**, *11*, 820.

(11) Ronen, A.; Walker, S. L.; Jassby, D. Electroconductive and electroresponsive membranes for water treatment. *Rev. Chem. Eng.* **2016**, *32*, 533−550.

(12) Formoso, P.; Pantuso, E.; De Filpo, G.; Nicoletta, F. Electro-Conductive Membranes for Permeation Enhancement and Fouling Mitigation: A Short Review. *Membranes* **2017**, *7*, 39.

(13) Agana, B. A.; Reeve, D.; Orbell, J. D. The influence of an applied electric field during ceramic ultrafiltration of post-electrodeposition rinse wastewater. *Water Res.* **2012**, *46*, 3574−3584.

(14) Enevoldsen, A. D.; Hansen, E. B.; Jonsson, G. Electro-ultrafiltration of industrial enzyme solutions. *J. Membr. Sci.* **2007**, *299*, 28−37.

(15) Gall, I.; Herzberg, M.; Oren, Y. The effect of electric fields on bacterial attachment to conductive surfaces. *Soft Matter* **2013**, *9*, 2443−2452.

(16) Dudchenko, A. V.; Rolf, J.; Russell, K.; Duan, W.; Jassby, D. Organic fouling inhibition on electrically conducting carbon nanotube−polyvinyl alcohol composite ultrafiltration membranes. *J. Membr. Sci.* **2014**, *468*, 1−10.

(17) Ronen, A.; Duan, W.; Wheeldon, I.; Walker, S.; Jassby, D. Microbial Attachment Inhibition through Low-Voltage Electrochemical Reactions on Electrically Conducting Membranes. *Environ. Sci. Technol.* **2015**, *49*, 12741−12750.

(18) Salvestrini, S.; Fenti, A.; Chianese, S.; Iovino, P.; Musmarra, D. Electro-Oxidation of Humic Acids Using Platinum Electrodes: An Experimental Approach and Kinetic Modelling. *Water* **2020**, *12*, 2250.

(19) Zhu, X.; Jassby, D. Electroactive Membranes for Water Treatment: Enhanced Treatment Functionalities, Energy Considerations, and Future Challenges. *Acc. Chem. Res.* **2019**, *52*, 1177−1186.

(20) Duan, W.; Ronen, A.; Walker, S.; Jassby, D. Polyaniline-Coated Carbon Nanotube Ultrafiltration Membranes: Enhanced Anodic Stability for In Situ Cleaning and Electro-Oxidation Processes. *ACS Appl. Mater. Interfaces* **2016**, *8*, 22574−22584.

(21) Li, C.; et al. Membrane fouling mitigation by coupling applied electric field in membrane system: Configuration, mechanism and performance. *Electrochim. Acta* **2018**, *287*, 124−134.

(22) Zhang, K.; Yang, Y.; Qiao, S.; Zhou, J.; Quan, X. Alternating current-enhanced carbon nanotubes hollow fiber membranes for membrane fouling control in novel membrane bioreactors. *Chemosphere* **2021**, *277*, No. 130240.

(23) Bhattacharjee, S.; Jassby, D.; Ramon, G. Z. The effect of an AC electric field on a colloidal particle near a permeable surface. *J. Membr. Sci.* **2024**, *709*, 123096.

(24) Hashemi Amrei, S. M. H.; Bukosky, S. C.; Rader, S. P.; Ristenpart, W. D.; Miller, G. H. Oscillating Electric Fields in Liquids Create a Long-Range Steady Field. *Phys. Rev. Lett.* **2018**, *121*, 185504.

(25) Bukosky, S. C.; Ristenpart, W. D. Simultaneous Aggregation and Height Bifurcation of Colloidal Particles near Electrodes in Oscillatory Electric Fields. *Langmuir* **2015**, *31*, 9742−9747.

(26) Woehl, T. J.; et al. Bifurcation in the steady-state height of colloidal particles near an electrode in oscillatory electric fields: Evidence for a tertiary potential minimum. *Phys. Rev. X* **2015**, *5*, 011023.

(27) Zumbusch, P. V.; Kulcke, W.; Brunner, G. Use of alternating electrical fields as anti-fouling strategy in ultrafiltration of biological suspensions - Introduction of a new experimental procedure for crossflow filtration. *J. Membr. Sci.* **1998**, *142*, 75−86.
(28) Ramon, G. Z.; Huppert, H. E.; Lister, J. R.; Stone, H. A. On the hydrodynamic interaction between a particle and a permeable surface. *Phys. Fluids* **2013**, *25*, 073103.
(29) Galvagno, M.; Ramon, G. Z. Hydrodynamic-Colloidal Interactions of an Oil Droplet and a Membrane Surface. *Langmuir* **2020**, *36*, 2858−2864.
(30) Wang, S.; Guillen, G.; Hoek, E. M. V. Direct Observation of Microbial Adhesion to Membranes †. *Environ. Sci. Technol.* **2005**, *39*, 6461−6469.
(31) Hashemi, A.; Miller, G. H.; Bishop, K. J. M.; Ristenpart, W. D. A perturbation solution to the full Poisin-Nernst-Planck equations yields an asymmetric rectified electric field. *Soft Matter* **2020**, *16*, 7052−7062.
(32) Segev-Mark, N.; et al. Colloidal deposition on polymer-brush-coated NF membranes. *Sep Purif Technol.* **2019**, *219*, 208−215.
(33) Itzhak, T.; et al. Atomic Layer Deposition for Gradient Surface Modification and Controlled Hydrophilization of Ultrafiltration Polymer Membranes. *ACS Appl. Mater. Interfaces* **2021**, *13*, 15591−15600.
(34) Fux, G.; Ramon, G. Z. Microscale Dynamics of Oil Droplets at a Membrane Surface: Deformation, Reversibility, and Implications for Fouling. *Environ. Sci. Technol.* **2017**, *51*, 13842−13849.
(35) Liu, Y.; Rosenfield, E.; Hu, M.; Mi, B. Direct observation of bacterial deposition on and detachment from nanocomposite membranes embedded with silver nanoparticles. *Water Res.* **2013**, *47*, 2949−2958.
(36) Kang, S.; Subramani, A.; Hoek, E. M. V.; Deshusses, M. A.; Matsumoto, M. R. Direct observation of biofouling in cross-flow microfiltration: mechanisms of deposition and release. *J. Membr. Sci.* **2004**, *244*, 151−165.
(37) Field, R. W.; Wu, D.; Howell, J. A.; Gupta, B. B. Critical flux concept for microfiltration fouling. *J. Membr. Sci.* **1995**, *100*, 259−272.
(38) Pollice, A.; Brookes, A.; Jefferson, B.; Judd, S. Sub-critical flux fouling in membrane bioreactors - A review of recent literature. *Desalination* **2005**, *174*, 221−230.
(39) Bacchin, P.; Aimar, P.; Field, R. W. Critical and sustainable fluxes: Theory, experiments and applications. *J. Membr. Sci.* **2006**, *281*, 42−69.

https://doi.org/10.1021/acs.estlett.5c00623
Environ. Sci. Technol. Lett. XXXX, XXX, XXX−XXX